ANNALS OF GEOPHYSICS, 67, 5, S551, 2024; doi:10.4401/ag-9120
OPEN ACCESS

Basement Neo-Tectonics of Western Himalayas from Seismic and Gravity Data Perspective

Mohammad Tahir[*,1], Bilal Saif[1], Tahir Iqbal[1], Raja Adnan Habib[1], Talat Iqbal[1], Muhammad Ali Shah[1]

(1) National Centre for Physics (NCP), Centre for Earthquake Studies (CES), Islamabad, Pakistan

Article history: received June 29, 2024; accepted October 31, 2024

Abstract

An earthquake of magnitude (Mw) 4.3 occurring on April 6, 2024 near Sargodha (Mianwali NW Punjab, Pakistan) has been analyzed through waveform inversion to understand the subsurface geological structure. This shallow-depth (19 km) event represents a strike-slip faulting with a dextral sense of movement. Gravity data of the epicentral area depicts distinct anomalies representing two separate blocks showing an off-set in the same direction as determined by the seismic inversion validating modeling results. In our opinion, these structures represent second-order tectonics, potentially emerging as a response to the hindrance caused by the Sargodha High to southward movement of the Himalayan deformation front. Alternatively, R-shears associated with the western boundary of the Indian plate could provide another explanation for such strike-slip mechanism events. Crustal shortening along the deformation front is being accommodated through aseismic slip along a viscous décollement in the Salt Range and seismic slip within the brittle basement rocks of the Sargodha region as represented by the analyzed seismic event. This dual process plays a key role in shaping the tectonic features in study area. Detailed studies of small to moderate seismic events can help in delineating the subsurface seismogenic structures for development of better seismo-tectonic model for realistic seismic hazard assessment in the region.

Keywords: Moment tensor inversion; Present day stress condition; Seismo-tectonic modeling

1. Introduction

Analysis of microseismic activity serves as a valuable tool for probing subsurface geological structures. This tool was used to study the buried seismogenic faults in the Sargodha region, located in the northwestern part of the Himalayan foreland. Several studies in the recent past have focused on examining surface and buried faults in the northern and central parts of the foreland. In these regions, thin-skinned tectonics is dominant, largely due to the presence of a weak Eocambrian salt layer acting as a décollement surface (Argand, 1922; Gansser, 1964; Powell and Conaghan, 1973; Seeber and Armbruster, 1979; Gansser, 1981; Jouanne et al., 2011; MonaLisa and Jan, 2012; Asim et al., 2014; Jadoon et al., 2021; Jouanne et al., 2020; Meyer et al., 2024). The subsurface geology and buried faults of the Sargodha region covered by thick terrigenous sands, remain largely unexplored. The recent earthquake occurrence emphasizes the importance of seismo-tectonic modeling, required for assessing future seismic hazards.

Gansser (1964) speculated on the basis of linear rock exposures of the Sargodha-Shahkot ridge that large desert tracts of northern Punjab are underlain by Indian Shield elements (Fig. 1). Following the classical gravity survey of Glennie (1932), Warsi and Molnar (1977) reported that the Bouguer anomaly of the Sargodha basement high is expressed through a positive gravity closure with an NW-SE trend, almost parallel to the central Himalaya.

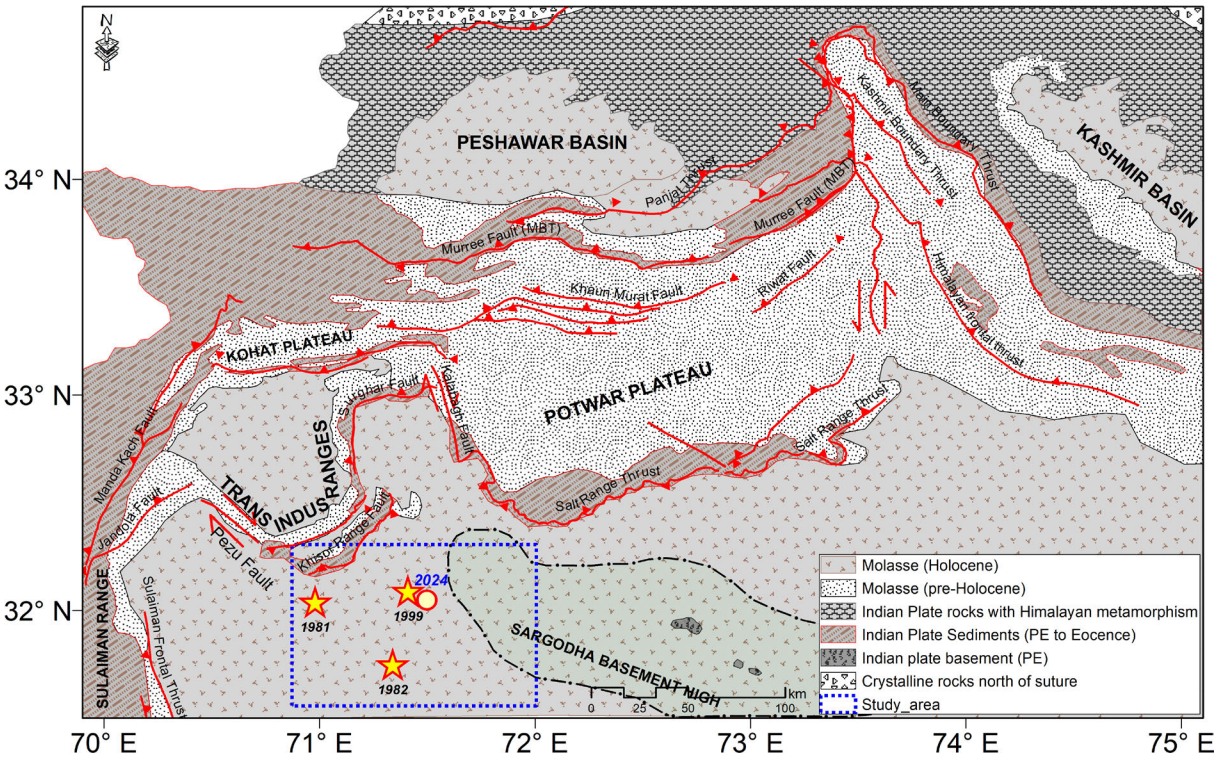

Figure 1. Regional geological map of the NW Himalayan foreland fold-and-thrust belt (modified from Blisniuk et al., 1998). Stars indicate location of events with a moment magnitude greater than 4.5, which occurred in 1981, 1982 and 1999. The filled circle represents the location of a recent event.

Farah et al. (1977; 1984) attributed the prominent positive gravity closures in the area to density contrast in the basement arising from igneous intrusions. Although the possibility of these intrusions cannot be ruled out, it was not possible to obtain a satisfactory fit to the positive gravity anomaly using this explanation. Therefore, an alternative description is required to account for the Bouguer anomaly that was observed over the Sargodha High. According to Bilham et al. (2003) this ridge seems to be a flexural bulge at the edge of the Himalayan foreland basin that formed in response to the downward bending of the Indian Plate due to its convergence with the Eurasian Plate. At the upper surface of the underthrusting tectonic plate, normal faults have been identified by gravity and seismic surveys. These normal faults, believed to be due to flexure of the lithosphere, offset the Precambrian basement. In the locality of these faults, the gravity gradient represents a northward dip (towards the downthrown block side). These normal faults terminate in pre-Siwalik formations, implying that these faults have not been active in Cenozoic time (Farah et al., 1977, 1984; Jaumé and Lillie, 1988; Irfan et al., 2005; Ahmad et al., 2023).

As far as strike-slip faulting is concerned, various explanations were suggested by different geoscientists for such faulting observed in this region (e.g., Crawford, 1974; Jaumé and Lillie, 1988; Cotton and Koyi, 2000; Faisal et al., 2015). Strike-slip faulting in the sedimentary cover is associated with relative movement of different parts of fold-and-thrust belt where eastern part i.e. Potwar Plateau and Salt Range slid further southwards due to a basal salt layer, while the western part (Kohat Plateau and Trans-Indus Salt Ranges) experienced more internal deformation due to the lack of salt (Crawford, 1974; Jaumé and Lillie, 1988; Cotton and Koyi, 2000; Faisal et al., 2015; Jouanne et al., 2020). In addition to salt tectonics, heterogeneous deformations along the strike of the Main Frontal Thrust (MFT) are thought to be due to some other factors like basement geometry, overburden geometry, or a combined effect of both (Abir et al., 2015; Jouanne et al., 2020).

This explanation seems to be valid for the sedimentary sequence above the basement; but strike-slip faults in shield rocks cannot be explained this way. In the western part, the ramping of frontal thrust may have been facilitated by the basement bend as the northeast edge of the Sargodha basement ridge converged with the overthrust belt (Leathers, 1987; Baker et al., 1988). The same interaction of the fold belt with the Sargodha ridge may be one of the possible reasons for the production of strike-slip faulting in the area under consideration. Another possibility has been discussed by Sercombe et al. (1998) suggesting that the basement strike-slip faults as well as the surface faults like Kalabagh and Pezu faults may be the R-shears of the left-lateral transform boundary i.e. Chaman Fault system. Other studies conducted in the northern region of the study area, such as surface geological maps of the Kohat Plateau, demonstrate structural characteristics are consistent with strike-slip faulting (Biddle and Christie-Blick, 1985; Pivnik and Sercombe, 1993). Magnetic and gravity data of the area also show conjugate sets of NW-SE and NE-SW basement-fault lineaments that coincide with some previous earthquake studies (e.g., Seeber et al., 1981; Verma and Sekhar, 1986; Sercombe et al., 1998). Furthermore, Seeber et al. (1981) marked three right-lateral strike-slip faults on the basis of micro-seismicity patterns in the south of MFT or SRT (Salt Range Thrust). However detailed analyses of these faulting styles using recent seismic data, stress build-up, strain accumulation, and their interactions were missing.

In this study, seismic waveform data from a local seismic network was utilized to analyze fault plane solutions of the April 6, 2024, Sargodha earthquake (Mw 4.3). For this purpose, seismic data from the Centre for Earthquake Studies (CES) and Pakistan Meteorological Department (PMD) have been utilized. These seismic networks offer excellent coverage with considerable azimuthal redundancy (Fig. 2). Additionally, epicentral parameters are

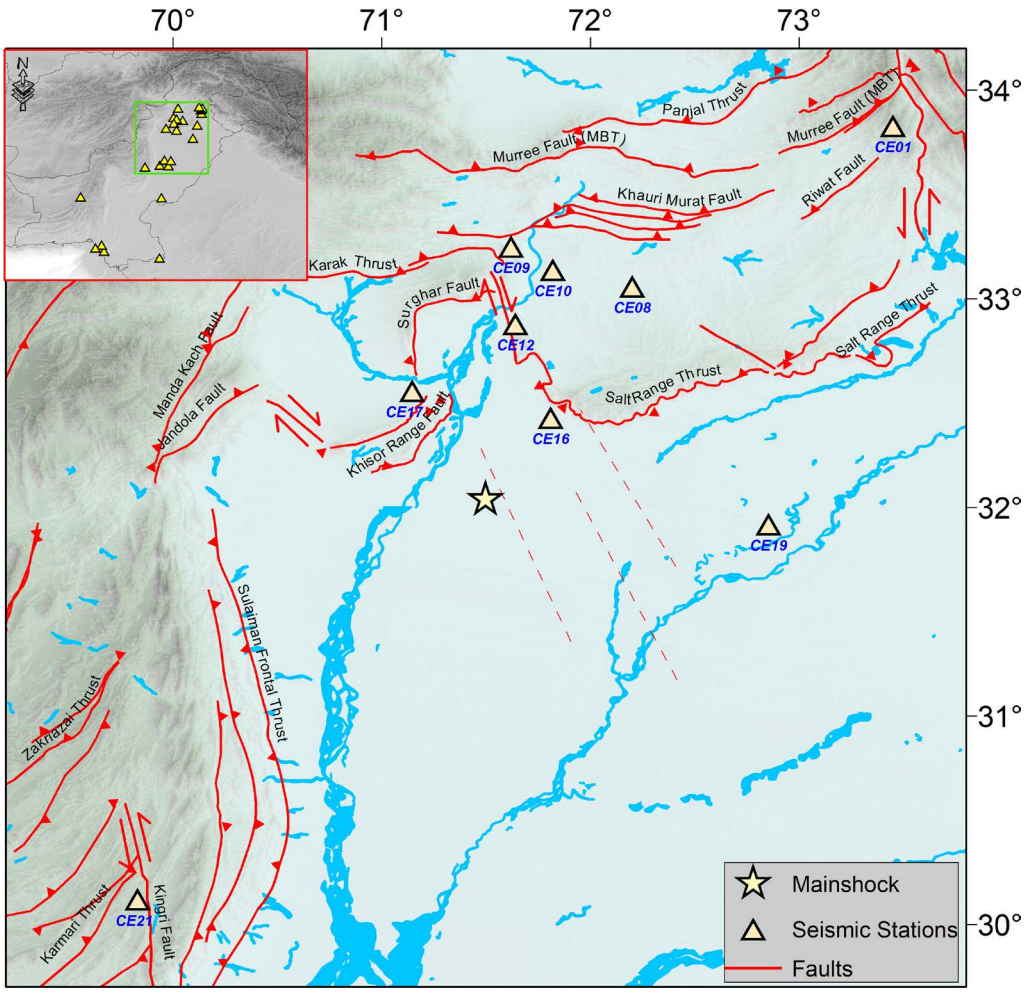

Figure 2. Location map of main shock of the Sargodha earthquake (star) with station (triangle) distribution of Centre for Earthquake Studies (CES) and Pakistan Metrological Department (PMD) that were used in moment tensor inversion. Inset figure show all stations of CES and PMD. Three dotted lines show the lineaments or fault zone marked by Seeber et al. (1981).

well determined from standard location techniques; but event depth is rarely known accurately. For accurate depth determination, either some additional phases of the event are required, or moment tensor inversion may be employed. Moment tensor inversion uses complete waveform to constrain hypocentral depth (Gilbert, 1971). Moreover, the moment tensor has a linear relation with fault orientation parameters (Stein and Wysession, 2002). Gravity data modeling helped us identify different fault types at varying depths and determine the strike direction of the fault planes. Hypocentral parameters and faulting style are prerequisites for seismo-tectonic studies and seismic hazard assessment of any area (Fig. 3).

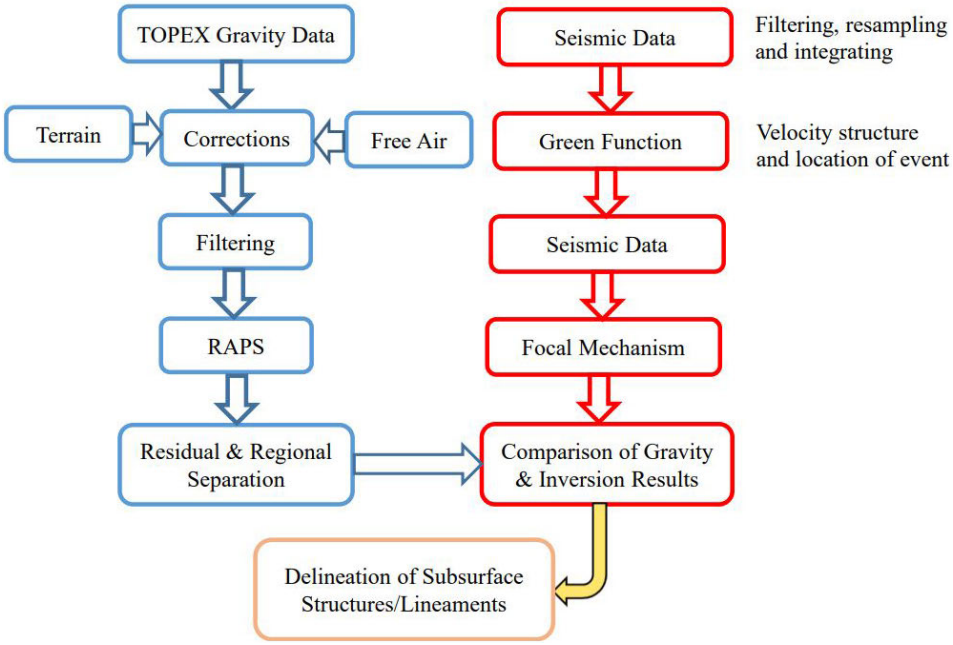

Figure 3. Illustrative flowchart depicting the data sources and methodological steps employed in this study.

2. Geology of the study region

The epicentral area lying at the eastern margin of Thal desert is a part of flood plain of River Jhelum. Geophysical surveys conducted for oil exploration suggest presence of a thick soil cover comprising of fluvial sand and silt that is underlain by sedimentary rock sequence up to a depth of more than a kilometer below which rocks of Indian Shield are present (Irfan et al., 2005). Shield rocks are exposed southeast of the epicenter, along the Kirana Hills which form outcrops of the most northwesterly Indian Shield elements. These rock outcrops are part of Sargodha-Shahkot Ridge and clearly indicate that the large desert tract of the northern Punjab is underlain by shield elements (Gansser, 1964; Ahmad et al., 2023).

The Sargodha-Shahkot ridge is a very interesting tectonic feature origin of which has been discussed extensively by a geological community working in this region for a long time. Gansser (1964) and Pasco (1959) related it with the North-South Aravali Range of India while others are of opinion that the ridge is in fact flexural bulge along the border of the Himalayas. The ridge extends for about 100 km from East to West in four separate groups (Kirana, Chiniot, Sangla and Shahkot). Their steeply rising topography and the intense black desert coating of the serrated ridges are impressive features. The predominant rocks are hardened grey-greenish shales and metasedimentary rocks including slates containing small biotites and coarse-to fine-grained reddish quartzites. Both the slates and the quartzites, are accompanied by small bands of diabase together with thin layers of rhyolites and rhyolitic tuffs. In the eastern part, the Shahkot Ridge takes an abrupt change in a strike of 90° and gets parallel to regional trend of the Aravalli Range of India. For this reason, the Shahkot Ridge is thought to be the western part of Aravalli Range (Gansser,1964). The sediments of the Kirana Hills are comparable with those of the Ajabgarh division of the Delhi system, or with the Malani group of Aravalli (Pascoe, 1959).

3. Data and Method

3.1 Moment Tensor inversion

Moment tensor inversion was performed for the Sargodha earthquake (Mw 4.3) to determine the focal mechanism solution. The main advantage of this technique (moment tensor inversion) is its utilization of full waveform data and modeling source parameters (e.g., strike, dip, rake, and depth) based on the best waveform fitting between observed and synthetic data. To ensure consistent results for fault plane solutions and focal depth, stations exhibiting high noise levels or experiencing time or amplitude issues were discarded. Seismic Analysis Code (SAC) was used to process waveform data. A band pass filter between 0.07 and 0.1 Hz was employed to remove near-subsurface effects from source data (e.g., Fukuyama and Dreger, 2000). Seismic data were further corrected for instrument response, trend, and mean were removed. The computation of Green's function at various depths and stations is required for synthetic seismogram generation, which depends on the velocity structure and seismic wave propagation within the crust. A Green's function was computed using a discrete wave number technique developed by Kohketsu (1985). The fault plane solution is strongly dependent on the velocity structure and the anisotropic properties of the earth surface (Vavryčuk 2005, 2014; Sabahat et al., 2022). To calculate Green's function, we adopted the local velocity structure established by Soomro et al. (2022). Their model was derived using data from the same seismic network employed in this study. Some recent studies used this model for source parameter estimation (Shaukat et al., 2023a, b; Tahir et al., 2024), while others have raised concerns about its limitations (e.g., Sabahat et al., 2022, 2024).

For determining the source parameters of the considered events, a moment tensor technique scheme developed by Yagi and Nishimura (2011) was employed. The source geometry was presented by six elements of the moment tensors. The unknown parameters (strike, dip, rake, and depth) were selected on the basis of best fit between synthetic and observed data. The waveform fitting and their variance reduction are strongly dependent on the amplitude and time shift between observed and synthetic seismograms. To maximize a cross-correlation between two signals and reduce variance reduction (Vr), some shifting of the waveforms was performed. Uniform weights were assigned to all seismograms during an inversion process. The best inverted (lowest Vr value) source parameters and their waveform fitting for different events that occurred in the Sargodha region are shown in Fig. 4.

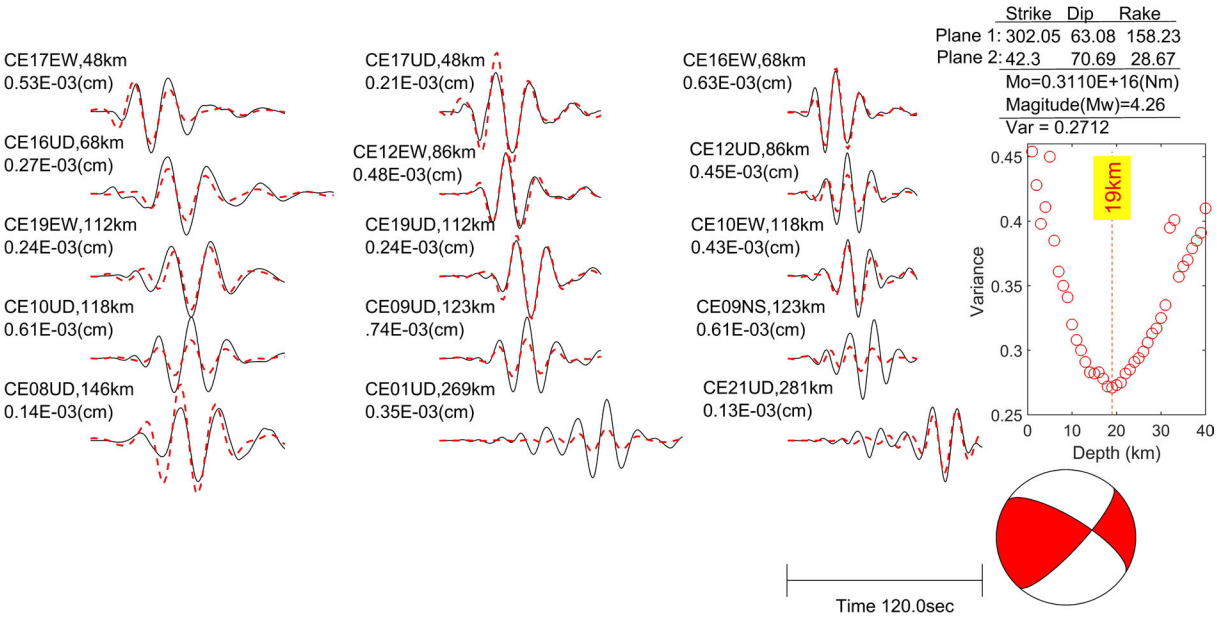

Figure 4 . Focal mechanism solution and depth inversion of April 4th 2024 Mw 4.3 earthquake obtained on the basis of waveform fitting between observed (solid lines) and synthetic (dotted lines) waveforms. Twelve components of ten stations were used to perform moment tensor inversion, a depth of 19 km through grid search and model parameters based on minimum variance reduction were obtained. Strike, slip and rake results are present on top right side of image. The NW-SE plane with 63o dip angle is taken as fault plane, which shows right lateral strike-slip mechanism.

3.2 Gravity Data Processing

Topographic and gravity data, in the form of Free Air Anomaly (FAA) for the region of a recent event and its surrounding area, were obtained from the TOPEX satellite (https://topex.ucsd.edu/cgibin/get_data.cgi). Bouguer and Terrain corrections were then applied to calculate the Complete Bouguer Anomaly (CBA), which collectively represents gravity/density variations at both residual and regional levels (Hackney et al., 2005; Maimuna et al., 2021; Salam et al., 2023). The Bouguer correction adjusts the Free Air Anomaly (FAA) for the influence of rock mass, utilizing a density value of 2670 kg/m3 (e.g., Parasnis, 1952; Siombone et al., 2021, 2022). The terrain correction approaches developed by Nagy (1966) and Kane (1962) were adopted in this study. Subsequently, the resulting CBA data underwent upward continuation before being separated into residual and regional levels. This step aimed to enhance the distinction between geological boundaries and subsurface anomalous sources (Layade et al., 2015).

The Radial Average Power Spectrum (RAPS) method was employed to differentiate between the residual and regional gravity responses (e.g., Spector and Grant, 1970; Chenrai et al., 2010; Ganguli et al., 2019; Basantaray and Mandal, 2022). This was achieved by plotting the logarithm of power against wavenumber. Initially, the CBA response underwent Fast Fourier transform (FFT) to obtain the spectrum (Chenrai et al., 2010). The plot was then segmented at a wavenumber (Wn) of 0.009, corresponding to an approximate depth of 40 km (determined from the slope segment), to separate gravity responses at the residual ($Wn > 0.009$) and regional ($Wn < 0.009$) levels (e.g., Guo et al., 2013; Zakariah et al., 2021). Additionally, a Butterworth filter with a cutoff of 8.5o was applied to further separate residual and regional gravity variations (e.g., Igwesi and Umego, 2013; Olokoba and Magaji, 2020).

4. Results

One event of magnitude (Mw) greater than 5.0 was observed in the available instrumental catalogs; whereas no historical earthquake has been documented in this region. The largest event in the area had a magnitude of 5.2 that occurred near the city of Bhakkar on May 5, 1982 (Fig. 1 and Table 1). The absence of large earthquakes and deep-buried geological structures under loose sand may cause difficulty in marking tectonic structures using surface geological techniques. In such cases small to moderate size events may be useful for delineating structures. However, establishing a spatial correlation between small earthquakes and specific faults is challenging due to inaccurate location, poor network coverage, strong heterogeneity of small structures, and the ill-posed conditions of moment tensor inversion.

No	Time (yyyymndy hr:min)	Location (degree)			Magnitude (Mw)
		Latitude	Longitude	Depth (km)	
1	19810720 1416	32.04	70.98	24	4.6
2	19820501 1742	31.75	71.34	35	5.2
3	19990911 2359	32.09	71.41	6	4.8
Abbreviations: year month day hour minutes, yyyymndy hr:min.					

Table 1. Source parameters of previously recorded seismic events with a magnitude (Mw) greater than 4.5, as shown in Fig. 1.

The source parameters of the Sargodha 6th April 2024 earthquake (Mw 4.3) were determined using the moment tensor inversion technique (Fig. 2). Nine seismic stations (15 different components of seismic stations) with azimuthal coverage for the event, more than 180o were selected. Model parameters (strike, dip, rake and depth of events) were obtained at the lowest variance reduction value. The best (lowest Vr ~ 0.27) waveform fitting between

observed and synthetic data for a recent event was achieved at a depth of 19 km. The fault plane solution of this event was strike-slip, with one nodal plane oriented in the NW-SE direction (Fig. 4). The strike direction of this event was consistent and had a trend in agreement with that of strike-slip faults marked by Seeber et al. (1981). It implies that the basement faulting may be the driving force for tectonic activities in the area. Earthquakes were shallow and primarily constrained to the basement with some earthquakes approaching the sedimentary cover over the basement.

The SW part of Pakistan consists dominantly of strike-slip events with principal stress axes oriented in the NW-SE direction (e.g., Shaukat et al., 2023b). Tectonically, strike-slip earthquakes can occur in various environments. The indentor or extrusion model can explain the tectonics of the Indian-Eurasian subduction. This model might be applicable in various geological scenarios, such as the North Anatolian fault or the Tibetan faults. However, in this case, it may not be suitable, as there haven't been sufficient observations of strike-slip faults to accommodate the extrusion or shortening (Chen et al., 2010).

4.1 Gravity data analysis

The variations in gravity data were incorporated to validate the results and tectonic interpretations derived from the focal mechanism solution of the selected event considered in this study. The variations in CBA values (−200 to +150 mGals), along with focal mechanism solutions and depth values of the corresponding events, are shown in Fig. 5. An anomalously high gravity region (> +80 mGals) was observed in the southeastern part of the study area. Furthermore, the northernmost region from the study area also depicts discrete anomalous parts (gravity values > +50 mGals). Our study area lies in the vicinity of a negatively anomalous region with gravity values ranging from 0 to −35 mGals, which is further surrounded by more negative gravity variations, ranging from −35 to −115 mGals, depicting the distinctions in structures. Know structures and faults (Sargodha High, Salt Range Thrust, Pezu Fault, Marwat Range, Khisor Range Fault) were robustly correlated with CBA gravity data (Fig. 5). Although, there are minor variations in CBA data in the vicinity of study area, but unable to be delineated prominently.

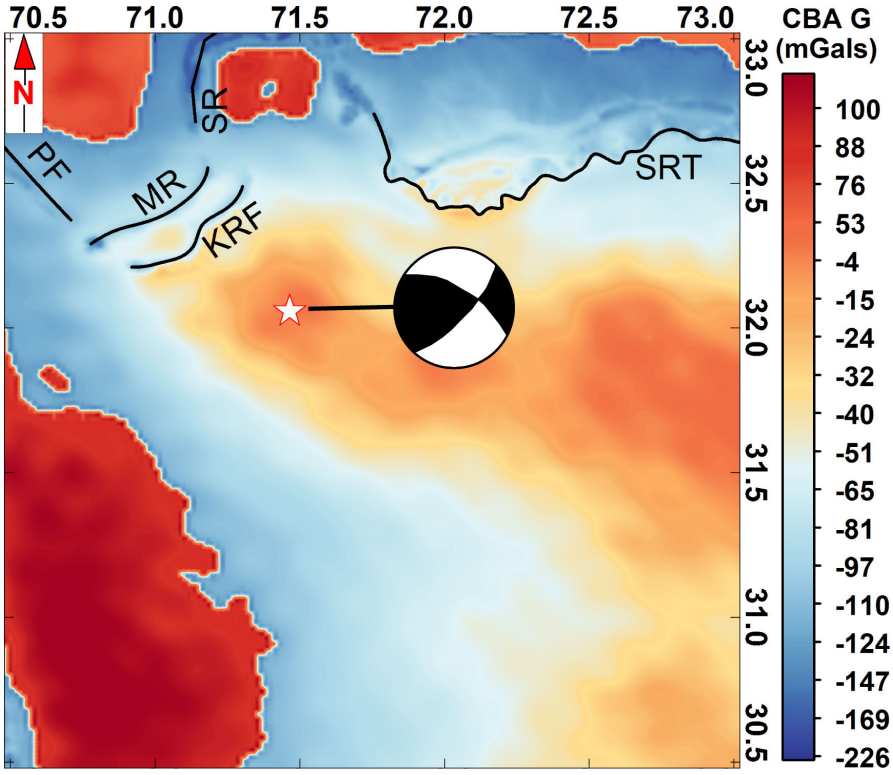

Figure 5. Complete Bouguer Anomaly (CBA) of the study area represents gravity variations collectively at residual and regional levels, with available focal mechanism solutions and their corresponding depths. SRT is Salt Range Thrust, PF is Pezu Fault, MR is Marwat Range, KRF is Khisor Range Fault.

Moreover, the residual plot (Fig. 6) identifies strike-slip faulting style, validating the inversion result (fault plane and depth). We marked lineaments, comprising three conjugated right-lateral strike-slip faults. Additionally, CBA delineated geological faults and structures were well resolved in residual gravity data responses.

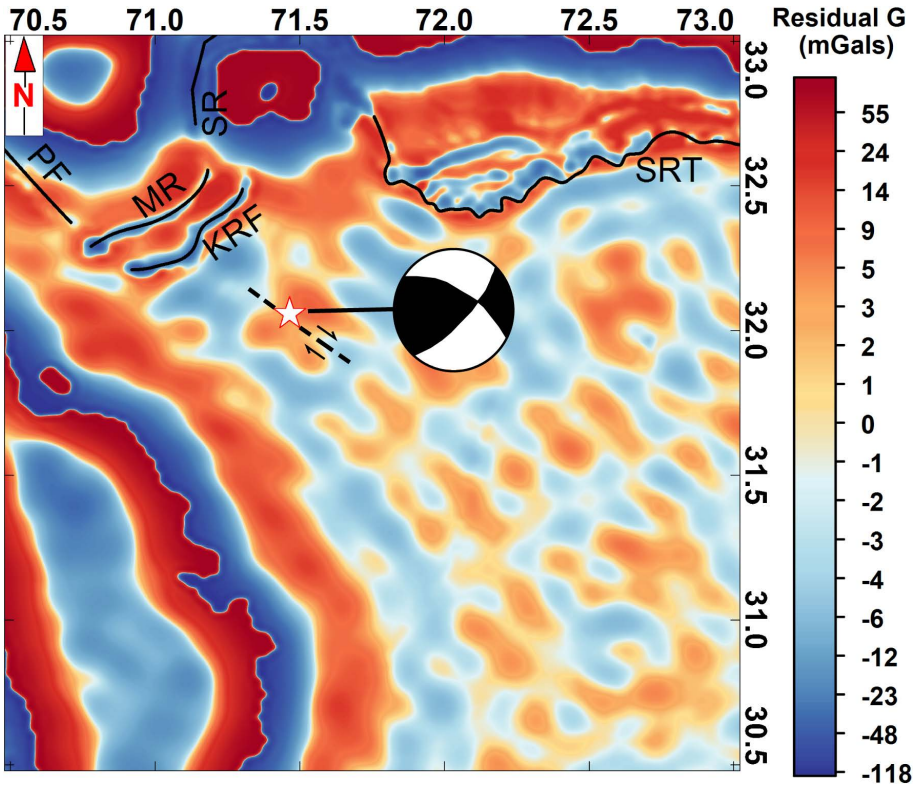

Figure 6. Residual gravity variations (depth < 40 km) of the study area, with strike-slip fault zone (lineaments) marked by dotted lines.

5. Discussion

Three possible scenarios could explain the occurrence of strike-slip faulting in the area. The Salt Range may play a vital role in the formation of strike-slip faults in this region. In the east and west of the Salt Range, salt thickness decreases compared to the central part (e.g., Abir et al., 2015). Thus, the friction coefficient of the substrate overburden sedimentary cover changes dramatically. A thick salt substrate is more ductile compared to a thin one (Cotton and Koyi, 2000). Consequently, the overburden over a ductile substrate propagates faster and farther to the south compared to a brittle substrate. This differential propagation might have caused the detachment of the western front in the Salt Range and formed the right-lateral Kalabagh fault. Shortening, folding, and clockwise rotation in overburden strata have been caused by transpressive movement along the Kalabagh fault. However, this model may not fully explain the occurrence of strike-slip in the basement. The cluster of strike-slip events in the recent analysis lies over the footwall of the Salt Range thrust and within the Punjab Foreland Basin. We speculate that the interaction of the fold belt with the basement ridge produced as a flexural bulge may be a reason for conjugate faulting in this region (Fig. 5).

These strike-slip events may accommodate the crustal thickening and shortening from north to south in the foreland. This is a typical feature of localized reentrants in the Himalayan foreland and thrust belt. Abir et al. (2015) reported that the lack of internal deformation in the hanging wall of SRT shows smooth transportation of overburdened strata. This may have further flexed the basement rock in an upward direction because of the hindrance offered by Sargodha high in the South of Salt Range Thrust. The same reason has probably caused anomalous uplifting of the southwestern bend of the Salt Range. These findings are in accordance with the gravity model of Farah et al. (1977) and this fact further supports the model of strike-slip faulting in the basement.

Another possibility has been discussed by Sercombe et al. (1998), which suggests that the basement strike-slip faults as well as the surface faults, like Kalabagh and Pezu faults may be the R-shears of the left-lateral transform boundary, i.e. the Chaman fault. We observed self-similarity over the fault zone (Fig. 5), as at any scale the fault sense of movement is similar (i.e. left-lateral). On a much larger scale, the geometry of the main fault is self-similar. On a local scale, the fault zone and subsidiary shears may follow the Reidel Shear model. The average principal stress axis seems to be acting in north-south direction, where fault strike is at an angle in NW direction. In compressional direction, we observe thrust component in source mechanisms of the event, which is in agreement with the Reidel shear model. Further in tension direction, there should be normal mechanism, i.e., the transpressional environment should change into tension in east-west direction. In our case, we have not observed normal mechanism events due to limited data, but previously, (Zoback, 1992; Heidbach et al., 2010) (in the world stress map) observed tension events on both sides of the study area that go in the favor of Reidel shear model. The left-lateral sub-faults that splay off the main fault represent R-shears.

Their presence suggests overall left-lateral motion in the zone. A cluster/parallel P-shear, has not been observed in this fault zone. This may be due to the fact that more stress is required for P-shear as compared to R-shear. (Pinar et al., 2003) suggest that 0.1 MPa and 0.5 MPa stress is required for $M > 4.0$ earthquake to trigger R- and P shears, respectively. Most researchers agree that R-shear develops first and P-shear develops later on; but in a specific environment, such as in a dilation system, both R- and P-shears develop simultaneously (Morgenstern and Tchalenko, 1967; Tchalenko, 1970; Bartlett et al., 1981). R-shear represents layers parallel to the simple shear direction, whereas P-shear is related to the shortening direction (Swanson, 1988, 1990). Accordingly, shortening may not happen along a fault plane. Studies carried out in the Kohat Plateau based on surface geology, reveal strike-slip faulting (Biddle and Christie-Blick, 1985; Pivnik and Sercombe, 1993). Gravity data in the study area show conjugate sets of NE-SW basement fault lineaments which coincide with some previous earthquake studies (Seeber and Armbruster, 1979; Seeber et al., 1980; Verma and Sekhar, 1986).

6. Conclusions

Seismo-tectonic analysis of Sargodha high region event was performed using local broadband waveform data from CES and PMD. This strike-slip event was relatively shallow (19 km depth) that occurred along NW-SE oriented fault, consistent with faults marked by that of Seeber et al. (1981). The residual gravity data also validates presence of shallow faults showing right lateral strike-slip movement. The formation of strike-slip faulting in the shield rocks seems to be a result of the interaction of the Himalayan fold-belt with basement high (Sargodha ridge) or R-shears of the western plate boundary, i.e. Chaman fault system. The crustal shortening may have been occurring partly aseismically along viscous decollement in the Salt Range and partly seismically within the brittle basement of the Sargodha region. However, role of uneven salt distribution in thin skinned tectonics cannot be ignored especially in case of shallower events in the topmost sedimentary layers. In future it is recommended to use additional data from inSAR and GPS for validation of seismic observations.

Data availability statement. The waveform data utilized in this study were obtained from PMD and are available upon request by contacting the corresponding author. Parametric data can be accessed at https://seismic.pmd.gov.pk/events.php. Topographic and gravity data, including Free Air Anomaly (FAA) values for the region of a recent seismic event and its surrounding area, were taken from the TOPEX satellite database (https://topex.ucsd.edu/cgibin/get_data.cgi).

Acknowledgments. The authors are obliged to the officials of CES and the PMD for providing data used in this work. We highly appreciate the support from CES collogues Naveed Mushtaq, Zafar Iqbal, and Muhammad Yousaf Khan. Their valuable suggestion improved figures quality and manuscript's technical writing. We thank Maria Teresa Mariucci, the editor-in-chief, and two anonymous reviewers for their valuable comments and suggestions, which have significantly improved this article.

References

Abdulnaby, W., H. Mahdi, H. Al-Shukri and N. Numan (2014). Stress patterns in Northern Iraq and surrounding regions from formal stress inversion of earthquake focal mechanism solutions, Pure Appl. Geophys., 171, 2137-2153, doi:10.1007/s00024-014-0823-x.

Abir, I. A., S. D. Khan, A. Ghulam and T. Shahina (2015). Active tectonics of western Potwar Plateau–Salt Range, northern Pakistan from InSAR observations and seismic imaging, Remote Sens. Environ., 168, 265-275, doi:10.1016/j.rse.2015.07.011.

Ahmad, B., S. H. Ali, A. Wahid and Y. Bashir (2023). Soft Sedimentary Deformations Structures (SSDS) in Neoproterozoic Sharaban Formation, Kirana Complex, Pakistan: Regional Tectonic Implications, Dokl. Earth Sci., 510, 371-386, doi:10.1134/S1028334X23600159.

Angelier, J. (1990). Inversion of field data in fault tectonics to obtain the regional stress-III. A new rapid direct inversion method by analytical means, Geophys. J. Int., 103, 363-376, doi:10.1111/j.1365-246X.1990.tb01777.x.

Angelier, J. (1984) Tectonic analysis of fault slip data sets, J. Geophys. Res., Solid Earth, 89, 5835-5848, doi:10.1029/JB089iB07p05835.

Angelier, J. and P. Mechler (1977). Sur une methode graphique de recherche des contraintes principales egalement utilisables en tectonique et en seismologie: la methode des diedres droits, Bull. Soc. Géol. Fr., 7, 1309-1318, doi:10.2113/gssgfbull.S7-XIX.6.1309.

Angelier, J., A. Tarantola, B. Valette and S. Manoussis (1982). Inversion of field data in fault tectonics to obtain the regional stress-I. Single phase fault populations: a new method of computing the stress tensor, Geophys. J. Int., 69, 607-621, doi:10.1111/j.1365-246X.1982.tb02766.x.

Argand, E. (1922). La tectonique de l'Asie. Conférence faite á Bruxelles, le 10 août 1922, In Rep. Sess., Int. Geol. Congr., 13, 170-372.

Asim, S., S. N. Qureshi and N. Khan (2014). Study of an uplift of Sargodha High by stratigraphical and structural interpretation of an east-west seismic profile in Central Indus Basin, Pakistan, Int. J. Geol., 5, 1027, doi:10.4236/ijg.2014.59088.

Baker, D. M., R. J. Lillie, R. S. Yeats, G. D. Johnson et al. (1988). Development of the Himalayan frontal thrust zone: Salt Range, Pakistan, Geology, 16, 3-7, doi:10.1130/0091-7613(1988)016<0003:DOTHFT>2.3.CO;2.

Barth, A. (2007). Frequency sensitive moment tensor inversion for light to moderate magnitude earthquakes in eastern Africa and derivation of the regional stress field, PhD thesis, University of Karlsruhe.

Bartlett, W., M. Friedman and J. Logan (1981). Experimental folding and faulting of rocks under confining pressure Part IX. Wrench faults in limestone layers, Tectonophysics, 79, 255-277, doi:10.1016/0040-1951(81)90116-5.

Basantaray, A. K. and A. Mandal (2022). Interpretation of gravity-magnetic anomalies to delineate subsurface configuration beneath east geothermal province along the Mahanadi rift basin: a case study of non-volcanic hot springs, Geotherm. Energy, 10, 6, doi:10.1186/s40517-022-00216-4.

Biddle, K. T. and N. Christie-Blick (1985). Strike-slip deformation, basin formation, and sedimentation, Soc. Econ. Pa., 37, 356, doi:10.2110/pec.85.37.

Bilham, R., R. Bendick and K. Wallace (2003). Flexure of the Indian plate and intraplate earthquakes, J. Earth Syst. Sci., 112, 315-329, doi:10.1007/BF02709259.

Blisniuk, P. M., L. J. Sonder and R. J. Lillie (1998). Foreland normal fault control on northwest himalayan thrust front development, Tectonics, 17, 766-779, doi:10.1029/98TC01870.

Blisniuk, P. M., L. J. Sonder and R. J. Lillie (1998). Foreland normal fault control on northwest Himalayan thrust front development, Tectonics, 17, 766-779, doi:10.1029/98TC01870.

Bohnhoff, M., S. Baisch and H. Harjes (2004). Fault mechanisms of induced seismicity at the superdeep German Continental Deep Drilling Program (KTB) borehole and their relation to fault structure and stress field, J. Geophys. Res., Solid Earth, 109, doi:10.1029/2003JB002528.

Chen, Y., J. Yu and S. Khan (2010). Spatial sensitivity analysis of multi-criteria weights in GIS-based land suitability evaluation, Environ. Model. Softw., 25, 1582-1591, doi:10.1016/j.envsoft.2010.06.001.

Cheng, W., Z. Zhang and X. Ruan (2009). Spatio-temporal variation and focal mechanism of the Wenchuan MS 8.0 earthquake sequence, Earthq. Sci., 22, 109-117, doi:10.1007/s11589-009-0109-z.

Chenrai, P., J. Meyers and P. Charusiri (2010). Euler deconvolution technique for gravity survey, J. Appl. Sci. Res., 6, 189-1897.

Cotton, J. T. and H. A. Koyi (2000). Modeling of thrust fronts above ductile and frictional detachments: Application to structures in the Salt Range and Potwar Plateau, Pakistan, Geol. Soc. Am. Bull., 112, 351-363, doi:10.1130/0016-7606(2000)112<351:MOTFAD>2.0.CO;2.

Crawford, A. R. (1974). The Salt Range, the Kashmir syntaxis and the Pamir arc, Earth Planet. Sci. Lett., 22, 371-379, doi:10.1016/0012-821X(74)90147-2.

Delvaux, D. (1993). The TENSOR program for paleostress reconstruction: examples from the east African and the Baikal rift zones, Terra Nova, 5, 216.

Delvaux, D. and A. Barth (2010). African stress pattern from formal inversion of focal mechanism data, Tectonophysics, 482, 105-128, doi:10.1016/j.tecto.2009.05.009.

Delvaux, D. and B. Sperner (2003). New aspects of tectonic stress inversion with reference to the TENSOR program, Geol. Soc. Spec. Publ., 212, 75-100, doi:10.1144/GSL.SP.2003.212.01.06.

Farah, A., G. Abbas, K. A. De Jong and R. D. Lawrence (1984). Evolution of the lithosphere in Pakistan, Tectonophysics, 105, 207-227, doi:10.1016/0040-1951(84)90204-X.

Farah, A., M. A. Mirza, M. A. Ahmed and M. H. Butt (1977). Gravity field of the buried shield in the Punjab Plain, Pakistan, Geol. Soc. Am. Bull., 88, 1147-1155, doi:10.1130/0016-7606(1977)88<1147:GFOTBS>2.0.CO;2.

Ganguli, S. S., S. Singh, N. Das, D. Maurya et al. (2019). Gravity and magnetic survey in Southwestern Part of Cuddapah Basin, India and its implication for shallow crustal architecture and mineralization, J. Geol. Soc. India, 93, 419-430, doi:10.1007/s12594-019-1196-7.

Gansser, A. (1964). Geology of the Himalayas, Wiley Interscience, New York.

Gansser, A. (1981). The geodynamic history of the Himalaya, Zagros Hindu Kush Himalaya Geodynamic Evolution, 3, 111-121, doi:10.1029/GD003p0111.

Gephart, J. W. (1990). Stress and the direction of slip on fault planes, Tectonics, 9, 845-858, doi:10.1029/TC009i004p00845.

Gilbert, F. (1971). Excitation of the normal modes of the Earth by earthquake sources, Geophys. J. Int., 22, 223-226, doi:10.1111/j.1365-246X.1971.tb03593.x.

Glennie, E. A. (1932). Gravity anomalies and the structure of the earth's crust, Geodetic Branch Office, Survey of India.

Guo, L., X. Meng, Z. Chen, S. Li et al. (2013). Preferential filtering for gravity anomaly separation, Comput. Geosci., 51, 247-254, doi:10.1016/j.cageo.2012.09.012.

Hardebeck, J. L. and E. Hauksson (2001). Crustal stress field in southern California and its implications for fault mechanics, J. Geophys. Res., Solid Earth, 106, 21859-21882, doi:10.1029/2001JB000292.

Heidbach, O., M. Tingay, A. Barth, J. Reinecker et al. (2010). Global crustal stress pattern based on the World Stress Map database release 2008, Tectonophysics, 482, 3-15, doi:10.1016/j.tecto.2009.07.023.

Horiuchi, S., G. Rocco and A. Hasegawa (1995). Discrimination of fault planes from auxiliary planes based on simultaneous determination of stress tensor and a large number of fault plane solutions, J. Geophys. Res., Solid Earth, 100, 8327-8338, doi:10.1029/94JB03284.

Igwesi, I. D. and N. M. Umego (2013). Interpretation of aeromagnetic anomalies over some parts of lower Benue Trough using spectral analysis technique, Int. J. Sci. Technol. Res., 2, 153-165.

Irfan, M., M. Shahid, M. Haroon and N. Zadi (2005). Sargodha high: a flexure forebuldge of the himalayan foreland basin, Geol. Bull. Univ. Peshawar, 38, 149-156.

Jadoon, I. A., L. Ding, S. R. K. Jadoon, Z. I. Bhatti et al. (2021). Lithospheric deformation and active tectonics of the NW Himalayas, Hindukush and Tibet, Lithosphere, 7866954, doi:10.2113/2021/7866954.

Jaumé, S. C. and R. J. Lillie (1988). Mechanics of the Salt Range-Potwar Plateau, Pakistan: A fold-and-thrust belt underlain by evaporates, Tectonics, 7, 57-71, doi:10.1029/TC007i001p00057.

Jouanne, F., A. Awan, A. Madji, A. Pêcher et al. (2011). Postseismic deformation in Pakistan after the 8 October 2005 earthquake: Evidence of afterslip along a flat north of the Balakot-Bagh thrust, J. Geophys. Res., 116, B07401, doi:10.1029/2010JB007903.

Jouanne, F., N. Munawar, J. Mugnier, A. Ahmed et al. (2020). Seismic Coupling Quantified on Inferred Décollements Beneath the Western Syntaxis of the Himalaya, Tectonics, 39, e2020TC006122, doi:10.1029/2020TC006122.

Kane, M. (1962). A comprehensive system of terrain corrections using a digital computer, Geophysics, 27, 455-462, doi:10.1190/1.1439044.

Kohketsu, K. (1985). The extended reflectivity method for synthetic near-field seismogram, J. Phys. Earth, 33, 2, 121-131, doi:10.4294/jpe1952.33.121.

Layade, G., B. Adebo, O. Olurin and O. Ganiyu (2015). Separation of Regional-Residual Anomaly Using Least Square Polynomial Fitting Method, J. Niger. Assoc. Math. Phys., 30, 169-180.

Leathers, M. R. (1987). Balanced structural cross section of the western Salt Range and Potwar Plateau, Pakistan: deformation near the strike-slip terminus of an overthrust sheet, M.S. thesis, 271, Dept. of Geology, Oregon State Univ., Corvallis, https://ir.library.oregonstate.edu/concern/graduate_thesis_or_dissertations/4q77ft72q.

Liang, C., Y. Yu, F. Wu F, L. Kang et al. (2021). Local stress field inverted for a shale gas play based on focal mechanisms determined from the joint source scanning algorithm, Earthq. Sci., 34, 222-233, doi:10.29382/eqs-2021-0003.

Lisle, R. J. (2013). A critical look at the Wallace-Bott hypothesis in fault-slip analysis, Bull. Soc. Géol. Fr., 184, 299-306, doi:10.2113/gssgfbull.184.4-5.299.

Maimuna, A. K., E. A. Pramesthi, Y. A. Segoro, R. Margiono et al. (2021). Analisis Anomali Gaya Berat Menggunakan Metode SVD dan Pemodelan 3D (Studi Kasus Gempa di Kepulauan Togean, Kabupaten Tojo Una-Una, Sulawesi Tengah), Jurnal Geofisika, 19, 17-23, doi:10.36435/jgf.v19i1.466.

Meyer, P., F. Jouanne, M. P. Doin, A. Awais et al. (2024). Present-day quantification of seismic coupling along the décollement level beneath the Potwar Plateau region in Pakistan western Himalaya, Earth Planet. Sci. Lett., 637, 118723, doi:10.1016/j.epsl.2024.118723.

Michael, A. J. (1984). Determination of stress from slip data: faults and folds, J. Geophys. Res., Solid Earth, 89, 11517-11526, doi:10.1029/JB089iB13p11517.

MonaLisa and M. Qasim Jan (2012). August 08, 2010, Sheikhupura, Pakistan earthquake: seismotectonic investigation using focal mechanism solution and gravity data, Nat. Hazards, 64, 397-403, doi:10.1007/s11069-012-0243-0.

Morgenstern, N. and J. Tchalenko (1967). Microscopic structures in kaolin subjected to direct shear, Geotechn., 309-328, doi:10.1680/geot.1967.17.4.309.

Nagy, D. (1966). The gravitational attraction of a right rectangular prism, Geophysics, 31, 362-371, doi:10.1190/1.1439779.

Olokoba, S. O. and Y. Magaji (2020). Analysis of high-resolution aeromagnetic data over parts of Sokoto basin, northwest Nigeria, Platform: A Journal of Engineering, 4, 14-30, doi:10.61762/pajevol4iss2art8601.

Parasnis, D. (1952). A study of rock densities in the English Midlands, Geophysical Supplements to the Monthly Notices of the Royal Astronomical Society, 6, 252-271, doi:10.1111/j.1365-246X.1952.tb03013.x.

Pinar, A., K. Kuge and Y. Honkura (2003). Moment tensor inversion of recent small to moderate sized earthquakes: implications for seismic hazard and active tectonics beneath the Sea of Marmara, Geophys. J. Int., 153, 133-145, doi:10.1046/j.1365-246X.2003.01897.x.

Pivnik, D. A. and W. J. Sercombe (1993). Compression-and transpression-related deformation in the Kohat Plateau, NW Pakistan, Geol. Soc. London, Spec. Pub., 74, 559-580, doi:10.1144/GSL.SP.1993.074.01.37.

Powell, C. M. and P. Conaghan (1973). Plate tectonics and the Himalayas, Earth Planet Sci. Lett., 20, 1-12, doi:10.1016/0012-821X(73)90134-9.

Rao, N. P., P. Kumar, T. Tsukuda and D. Ramesh (2006). The devastating Muzaffarabad earthquake of 8 October 2005: New insights into Himalayan seismicity and tectonics, Gondwana Res., 9, 365-378, doi:10.1016/j.gr.2006.01.004.

Reches, Z. (1987). Determination of the tectonic stress tensor from slip along faults that obey the Coulomb yield condition, Tectonics, 6, 849-861, doi:10.1029/TC006i006p00849.

Sabahat, S., M. Tahir, M. T. Iqbal, J. Iqbal et al. (2022). Source parameters of the Fatehjang, Pakistan earthquake (Mw 4.1) of 28 August 2020, Arab. J. Geosci., 15, 1-17, doi:10.1007/s12517-022-10919-4.

Sabahat, S., M. Tahir, F. Munir, B. Saif et al. (2024). Inversion techniques for focal mechanism determination of small-magnitude earthquakes a comparative study using the Burewala earthquake (Mw ~ 4) in Pakistan, J. Seismol., 28, 119-131, doi:10.1007/s10950-023-10186-0.

Seeber, L. and J. Armbruster (1979). Seismicity of the Hazara arc in northern Pakistan: decollement versus basement faulting, Geodynamics of Pakistan, Geol. Surv. Pakistan, Quetta, 131-147.

Seeber, L., J. G. Armbruster and R. C. Quittmeyer (1981). Seismicity and continental subduction in the Himalayan arc, Zagros Hindu Kush Himalaya Geodynamic Evolution, Wiley Online Library, 3, doi:10.1029/GD003p0215.

Seeber, L., R. Quittmeyer and J. Armbruster (1980). Seismotectonics of Pakistan: A review of results from network data and implications for the Central Himalaya, Geol. Bull. Univ. Peshawar, 13, 151-68, http://ojs.uop.edu.pk/jhes/article/view/1194.

Sercombe, W. J., D. A. Pivnik, W. P. Wilson, M. Albertin et al. (1998). Wrench faulting in the northern Pakistan foreland, Bull. Am. Assoc. Petr. Geol., 82, 2003-2030, doi:10.1190/1.1932005.

Shaukat, A. Z., M. Tahir, T. Iqbal, T. Iqbal et al. (2023a). Seismotectonic Analysis of the 7 October 2021 M w 5.9 Harnai Earthquake, Pakistan, Bull. Seismol. Soc. Am., 113, 636-647, doi:10.1785/0120220104.

Shaukat, A. Z., M. Tahir, T. Iqbal, T. Iqbal et al. (2023b). Seismic Interactions Between Northern Terminus of Ornahc-Nal and Hoshab Faults Based on Source Mechanism Investigation of 06 May 2022 Mw 5.4 Khuzdar Earthquake, Pure Appl. Geophys., 180, 3435-3455, doi:10.1007/s00024-023-03352-5.

Siombone, S., W. Jufri and M. Maba (2021). Land Cover, Land Surface Temperature and Geomorphology Structure at Tulehu Geothermal Area, Ambon, Indonesia, Int. J. Innov. Res. Sci. Eng. Technol., 8, 279-292.

Siombone, S. H., A. Susilo and S. Maryanto (2022). Integration of Topex Satellite Gravity and DEM SRTM Imagery for Subsurface Structure Identification at Tiris Geothermal Area, Lamongan Volcano Complex, Probolinggo, East Java, POSITRON, 12, 98-111, doi:10.26418/positron.v12i2.56880.

Spector, A. and F. Grant (1970). Statistical models for interpreting aeromagnetic data, Geophysics, 35, 293-302, doi:10.1190/1.1440092.

Stein, S. and M. Wysession (2002). An Introduction to Seismology, Earthquakes and Earth Structures, Wiley-Blackwell, 512, doi:10.5860/choice.40-4625.

Swanson, M. T. (1990). Extensional duplexing in the York Cliffs strike-slip fault system, southern coastal Maine, J. Struct. Geol., 12, 499-512, doi:10.1016/0191-8141(90)90037-Y.

Swanson, M. T. (1988). Pseudotachylyte-bearing strike-slip duplex structures in the Fort Foster Brittle Zone, S. Maine, J. Struct. Geol., 10, 813-828, doi:10.1016/0191-8141(88)90097-1.

Tahir, M., Z. Ahmad, S. Sabahat, M. N. Mushtaq et al. (2024). Source parameters and aftershock pattern of the October 7, 2021, M5. 9 Harnai earthquake, Pakistan, Earthq. Sci., 37, 4, 304-323, doi:10.1016/j.eqs.2024.04.007.

Tchalenko, J. (1970). Similarities between shear zones of different magnitudes, Geol. Soc. Am. Bull., 81, 1625-1640, doi:10.1130/0016-7606(1970)81[1625:SBSZOD]2.0.CO;2.

Vavryčuk, V. (2005). Focal mechanisms in anisotropic media, Geophys. J. Int., 161, 334-346, doi:10.1111/j.1365-246X.2005.02585.x.

Vavryčuk, V. (2014). Iterative joint inversion for stress and fault orientations from focal mechanisms, Geophys. J. Int., 199, 69-77, doi:10.1093/gji/ggu224.

Verma, R. and C. C. Sekhar (1986). Focal mechanism solutions and nature of plate movements in Pakistan, J. Geodyn., 5, 331-351, doi:10.1016/0264-3707(86)90013-X.

Warsi, W. and P. Molnar (1977). Gravity anomalies and plate tectonics in the Himalaya, Himalaya, Sciences de la Terre, 463-473.

Xu, Z., Z. Huang, L. Wang, M. Xu et al. (2016). Crustal stress field in Yunnan: implication for crust-mantle coupling, Earthq. Sci., 29, 105-115, doi:10.1007/s11589-016-0146-3.

Yagi, Y. and N. Nishimura (2011). Moment tensor inversion of near source seismograms, Bull. Int. Inst. Seismol. Earthq. Eng., 45, 133-138, https://api.semanticscholar.org/CorpusID:221606656.

Zakariah, M. N. A., N. Roslan, N. Sulaiman, S. C. H. Lee et al. (2021). Gravity analysis for subsurface characterization and depth estimation of Muda River Basin, Kedah, Peninsular Malaysia, Appl. Sci., 11, 6363, doi:10.3390/app11146363.

Zoback, M. L. (1992). First-and second-order patterns of stress in the lithosphere: the world stress map project, J. Geophys. Res., 97, B8, 11703-11728, doi:10.1029/92JB00132.

***CORRESPONDING AUTHOR: Mohammad TAHIR**,
National Centre for Physics (NCP), Centre for Earthquake Studies (CES), Islamabad, Pakistan
e-mail: mtyousafzai@gmail.com